ISSN 0001-4338, Izvestiya, Atmospheric and Oceanic Physics, 2019, Vol. 55, No. 9, pp. 949–955. © Pleiades Publishing, Ltd., 2019.
Russian Text © The Author(s), 2018, published in Issledovanie Zemli iz Kosmosa, 2018, No. 6, pp. 3–12.

PHYSICAL FOUNDATION OF EARTH OBSERVATION AND REMOTE SENSING

Testing the Algorithm for Determining the Near-Water Wind Direction Field Using Satellite Radiopolarimetric Measurements

D. S. Sazonov[a], *, V. V. Sterlyadkin[a, b], and A. V. Kuzmin[a]

[a]*Space Research Institute, Russian Academy of Sciences, Moscow, 117997 Russia*
[b]*Russian Technological University (MIREA), Moscow, 119454 Russia*
**e-mail: sazonov_33m7@mail.ru*

Received February 28, 2018

Abstract—The original MicRAWinD (Microwave Radiometric Algorithm for Wind Direction retrieval) algorithm planned for use in reconstructing the near-surface wind direction in the Convergence space experiment (SE) is presented. The possibility of determining the wind direction based on radiometric measurements in two swaths of the radiometer stems from the anisotropy of surface radiation, which is manifested most clearly in the third Stokes parameter. Combining the results of measurements at different frequencies with their reliability factored in, one can improve the accuracy of reconstructing the wind direction. A new algorithm for enhancing the reliability of measurements which takes the real errors in measuring brightness temperatures into account is proposed. The algorithm has been tested with real data provided by the WindSat radiometric system. The results are compared with the Remote Sensing Systems (RSS) reconstruction data. A surface region with different geophysical parameters (sea surface temperature, vapor content, wind speed and direction, and cloud water content) is chosen for this comparison. The reconstruction algorithm involves solving the direct problem of calculating the radio brightness temperatures at linear ±45° polarizations with subsequent calculations of the third Stokes parameter for 37, 18.7, and 10.7 GHz. The initial meteorological parameters for the direct problem are products provided by RSS. The sensitivity of radiometric instruments is taken into account in the simulation process. The solution of the inverse problem and the comparison results demonstrate that this algorithm retrieves the wind direction with fine qualitative agreement both from the results of radiometric observations at a single frequency and from multifrequency data.

Keywords: remote sensing, radio brightness temperature, azimuthal anisotropy, microwave radiometer, microwave radiation, modeling, wind speed and direction, Convergence space experiment

DOI: 10.1134/S0001433819090457

INTRODUCTION

Data obtained by Earth remote sensing (ERS) satellites have become crucial for climate research, weather forecasting, disaster prevention, and ecological monitoring, and they have various other practical applications. Remote measurements are performed in different frequency ranges (optical, infrared (IR), and microwave) with the use of active and/or passive observation techniques. Microwave radiometry has been proven efficient in global monitoring of the ocean–atmosphere system. This ERS instrument allows one to perform day-and-night measurements; features relatively low radiation absorption in the atmospheric “transparency windows”; and, most importantly, is highly informative.

Among all the microwave frequencies used for remote sensing (RS), three frequencies (~10, 18, and 37 GHz) localized in the “transparency windows” are exactly the ones at which the measured upward-travelling radio radiation is associated closely with the near-water wind field. This provides a unique opportunity to determine the wind parameters remotely. A large number of algorithms for determining the near-surface wind field have already been developed, but the reconstruction efficiency remains an issue. Although this is a matter of present interest, no Russian instruments are involved in experiments on determining the vector of near-surface wind in the ocean.

The full title of the Convergence space experiment (SE) aboard the Russian Orbital Segment (ROS) is “Determination of Detailed Atmospheric Temperature and Humidity Profiles in the Study of the Origin of Atmospheric Cataclysms.” The aim of Convergence is to examine the genesis and evolution mechanisms of large-scale catastrophic atmospheric processes (such as tropical cyclones or midlatitude hurricanes) as the key elements in the process of formation of the global mass and moisture exchange in the ocean–atmosphere system (Sharkov, 2017).

Determining the wind speed and direction through measurements of the own radiothermal emission of the water surface is one objective of the Convergence SE.

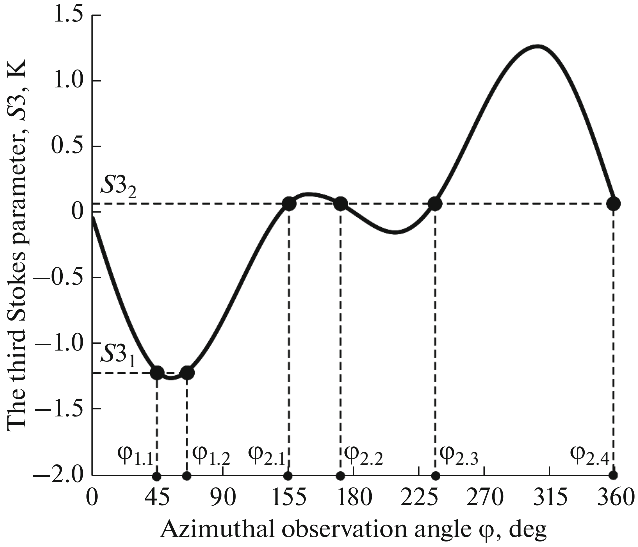

Fig. 1. Dependence of the third Stokes parameter ($S3$) on the relative wind azimuth. Two values ($S3_1$ and $S3_2$) are determined at two different sensing azimuths for the same surface element, and these two values are then used to find the sets of possible wind directions.

This SE should help optimize the algorithms of reconstruction of the near-water wind speed and direction and develop the necessary software. The measurement results are planned to be validated by comparing them to independent meteorological data and data from other sensors (Sadovsky and Sazonov, 2017).

The algorithm of reconstructing the near-surface wind direction based on satellite microwave polarimetric measurements has already been developed. It was applied to a model problem and demonstrated to be efficient (Sterlyadkin et al., 2017). It seems logical to test it using real satellite measurement data. As was already noted, the Convergence SE is still at the planning stage. Among all the current satellite radio polarimeters, only the WindSat instrument satisfies the requirements (see below) imposed by the mentioned algorithm for determining the wind direction. Therefore, the aim of the present study is to demonstrate the capabilities of the proposed algorithm using WindSat data as an example.

STATISTICAL ALGORITHM FOR ENHANCING THE RELIABILITY OF MEASUREMENTS AND THE USE OF DIFFERENT FREQUENCY CHANNELS

The possibility of determining the wind direction based on radiometric measurements stems from the azimuthal anisotropy of microwave radiation of a rough water surface. The effect of azimuthal anisotropy consists of the dependence of the measured radio brightness temperature on the angle between the wind direction and the sensing direction. This effect has been discovered by researchers from the Space Research Institute in the 1970s in experiments on radiothermal sensing of the sea surface by radiometric systems with nadir antennas installed aboard a testbed aircraft (Bespalova et al., 1979, 1982).

It was found that the third Stokes parameter ($S3$) is affected most by surface radiation anisotropy (Bespalova et al., 1979, 1982; Meissner and Wentz, 2012; Sazonov et al., 2013). This parameter is the difference of brightness temperatures at linear ±45° polarizations: $S3(\varphi, ...) = T_B^{+45}(\varphi, ...) - T_B^{-45}(\varphi, ...)$. The anisotropic contribution depends both on the radiation frequency and the magnitude of wind speed U_{10} (Meissner and Wentz, 2012; Sazonov et al., 2013; Sazonov, 2017). When reconstructing wind direction α_w, we assume that the magnitude of wind speed U_{10} is known from additional sources (e.g., scatterometer measurements) or was determined based on measurement data (Sadovsky and Sazonov, 2017). Therefore, the dependence of $S3$ on wind direction φ relative to sensing azimuth φ_s ($\varphi = \varphi_w - \varphi_s$) is also assumed to be known. The typical $S3(\varphi)$ dependence for frequency f_1 = 36.5 GHz is shown in Fig. 1.

It can be seen that the value of relative wind azimuth φ is ambiguous at any measured $S3$. Two angles $\varphi_{1.1}$ and $\varphi_{1.2}$ correspond to the $S3_1$ value in Fig. 1, and four possible angles $\varphi_{2.1}$, $\varphi_{2.2}$, $\varphi_{2.3}$, and $\varphi_{2.4}$ correspond to $S3_2$. It is impossible to determine in a single measurement which φ value represents the true wind direction. However, if one and the same element of resolution on the surface is measured at different angles, it becomes possible to identify the true direction.

Figure 2 presents the tentative geometry of conical sensing with the satellite moving along a track. The proposed algorithm may be applied to different satellite radiometers if measurements in two swaths are available. WindSat belongs to this group of instruments (Gaiser et al., 2004).

It follows from Fig. 2 that, if the initial forward sensing direction makes angle φ_{31}, the same element of resolution will be measured at angle $\varphi_{32} = \varphi - \varphi_{31}$ in aft sensing along the track. The difference between the sensing directions is $\Delta\varphi = \varphi_{32} - \varphi_{31} = \pi - 2\varphi_{31}$.

Naturally, the same element of resolution on the surface falls within the aft observation sector after the satellite covers distance $L(\varphi_{31}) = 2R\cos(\varphi_{31})$, where R is the radius of the scan cone on the surface of the Earth along the track. This displacement takes place with time delay $\Delta t = L/V$, where V is the satellite flight speed.

Thus, the same element of the underlying surface is measured at angles φ_{31} and $\varphi_{32} = \pi - \varphi_{31}$. Solving the inverse problem, we obtain two values of the third Stokes parameter ($S3_1$ and $S3_2$) and azimuthal viewing angles φ_{31} and φ_{32}. In Fig. 1, the initial wind direction is φ_w = 28°, sensing direction φ_{31} = −37°, and $\varphi_{32} = \pi - \varphi_{31}$ = −147°.

The MicRAWinD algorithm, which was described in (Sterlyadkin et al., 2017), is proposed to be used to reconstruct the wind direction based on the measured values of the third Stokes parameter.

Measurements of the intrinsic radiothermal radiation of the water surface are normally performed at several different frequencies instead of a single one. This is done to increase the reliability of measurements. We propose combining the results in different frequency channels with the measurement errors and the errors of indirect calculations taken into account. It is natural to assume that the signal distribution over the third Stokes parameter is a normal one and the width of this distribution corresponds to the errors of its calculation.

The algorithm of determining the wind direction relies on data on the geophysical parameters of the ocean–atmosphere system and the satellite telemetry. The meteo parameters are integral water-vapor content V, cloud water content L, precipitation rate R, wind speed U_{10} (at a height of 10 m), water temperature T_s, and salinity S. The Earth incidence angle (EIA), flight direction φ_f at a given moment, and the sensing direction relative to the flight direction are among the telemetry parameters. These parameters are needed to model the angular dependence (theoretical) of the third Stokes parameter ($S3$).

A random noise component, which is governed by the sensitivity of radiometers, and errors of determination of the wind speed magnitude, which is determined based on a set of measured brightness temperatures in the process of solving the inverse problem, are always present in actual radiometric systems. In addition, the model may also have errors. In this study, we consider only the radiometer noise, since it was estimated (Sadovsky and Sazonov, 2017) to produce the greatest contribution to the overall error. Owing to errors of measurement of brightness temperatures, the true values of the third Stokes parameter may differ from the measured $S3_1$ and $S3_2$ values. Therefore, the statistical distribution of probabilities should be taken into account.

With the statistical distribution factored in, the following algorithm is proposed for reconstructing the wind direction based on the results multifrequency measurements of the third Stokes parameter.

(1) The theoretical azimuthal angular dependence of the third Stokes parameter is calculated for the known (determined beforehand) geophysical parameters of the ocean–atmosphere system and the satellite telemetry (Fig. 1):

$$S3(\varphi,\ldots) = T_B^{+45}(\varphi,\ldots) - T_B^{-45}(\varphi,\ldots),$$

where $T_B(\varphi, \ldots)$ is the radio brightness temperatures at linear ±45° polarizations.

(2) The probability distribution functions over $S3$ ($P_1(S3, \mu_1, \sigma)$ and $P_2(S3, \mu_2, \sigma)$) are formed for the

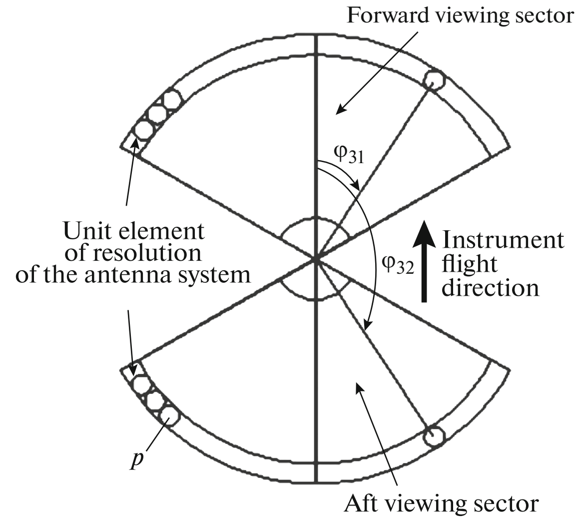

Fig. 2. Geometry of sensing of the same surface elements by a satellite moving along the track.

first and second measurements. Probability function P corresponds to a normal distribution with standard deviation $\sigma = \delta_{S3} = \sqrt{2}\delta_p$, where δ_r is the radiometer sensitivity in a given frequency channel, and mean values equal to the measured values the third Stokes parameter ($\mu_1 = S3_1$ and $\mu_2 = S3_2$).

(3) Probability functions $P_i(\varphi)$ are calculated. $P_i(\varphi)$ is the probability that the true wind direction at a measured $S3_i$ value has relative azimuthal angle φ: $P_i(\varphi) = P_i(S3_i, \mu_i, \sigma)$, where $i = 1, 2$. The probabilities are calculated for discrete angle values φ_j, where $j = 1–360$ (Fig. 3).

(4) Probability functions $P_1(\varphi)$ and $P_2(\varphi)$ are normalized:

$$P_N(\varphi) = \frac{P(\varphi)}{\sum_j P(\varphi)}.$$

Normalized probabilities are used in what follows.

(5) The plots for probabilities $P_1(\varphi)$ and $P_2(\varphi)$ are shifted in angle to the zero sensing azimuth. Dependences $P_1(\varphi + \varphi_{31})$ and $P_2(\varphi + \varphi_{32})$ are thus obtained (Fig. 4).

(6) The overlapping of probabilities is determined for a single channel:

$$P_O(\varphi_w) = P_1(\varphi + \varphi_{31})P_2(\varphi + \varphi_{32}).$$

The wind direction is then determined as the maximum value: $\varphi_w = \max(P_O(\varphi_w))$ (Fig. 4).

(7) This algorithm is applied to all frequency channels measuring the third Stokes parameter. The wind direction is determined by identifying the maximum of the resulting probability function for all channels:

$$P_{res}(\varphi_w) = C1P_{O1}(\varphi_w) + C2P_O(\varphi_w) + C3P_O(\varphi_w),$$

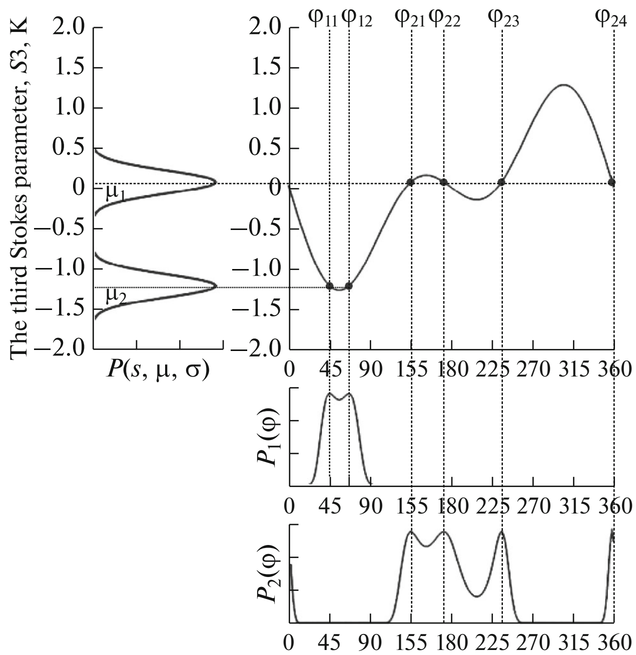

Fig. 3. Probability functions $P_1(\varphi)$ and $P_2(\varphi)$ define the probability that the true relative wind azimuth is φ under the condition that the measured values of the third Stokes parameter are $S3_1$ and $S3_2$. The initial wind direction is taken to be $\varphi_w = 28°$, sensing direction φ_{31} is $-37°$, and $\varphi_{32} = -147°$. For clarity, σ is set to 0.1 K (the actual sensitivity of WindSat at 37 GHz is 0.25 K).

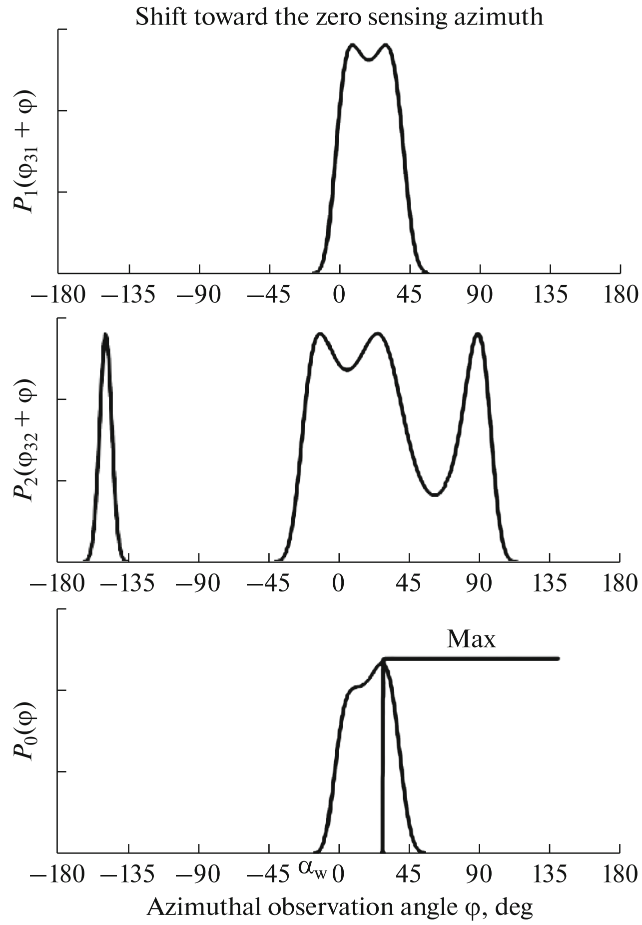

Fig. 4. Plots of probabilities $P_1(\varphi_{31} + \varphi)$ and $P_2(\varphi_{32} + \varphi)$ shifted to the zero sensing azimuth and overall probability $P_O(\varphi_w)$. The wind direction corresponds to the maximum: $\varphi_w = \max(P_O(\varphi))$.

where C1, C2, and C3 are weight coefficients representing the reliability of measurements in a given radiometric channel.

Applying the proposed signal processing algorithm, one determines wind direction φ_w relative to the satellite track direction as the angle at which the $P_O(\varphi)$ probability function is maximized (Fig. 4). The combination of resulting probabilities in different channels makes the solution more stable. However, this data aggregation should be done with the reliability of channel measurements taken into account. One may use, e.g., the anisotropic signal/noise ratio in each radiometric channel as a weight coefficient.

RECONSTRUCTING THE WIND DIRECTION BASED ON SATELLITE MEASUREMENTS

Among all the microwave instruments aboard artificial satellites, only WindSat performs measurements in the complete polarimetric basis (i.e., measures all four Stokes parameters). This instrument is currently (February 2018) in operation aboard the Coriolis satellite, which was launched in 2003. Its scan geometry (Fig. 5) is such that measurements for the ocean–atmosphere system are conducted both in the flight direction and in the opposite direction.

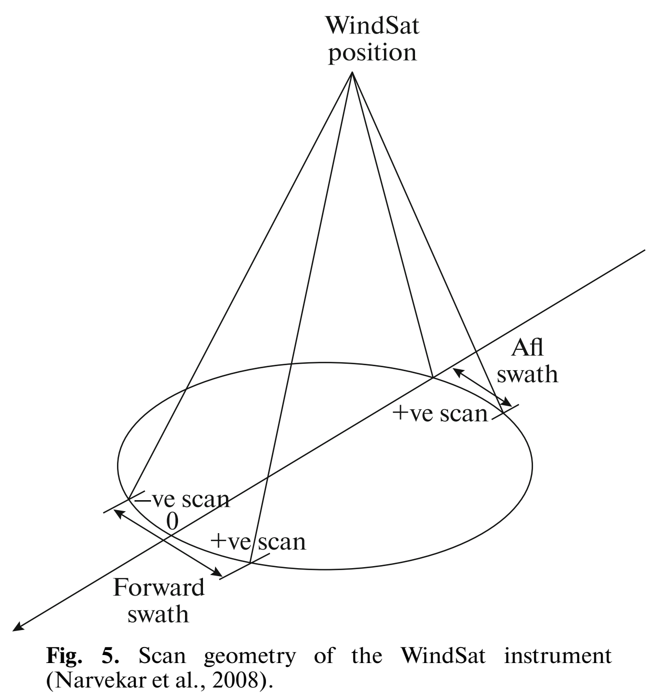

Fig. 5. Scan geometry of the WindSat instrument (Narvekar et al., 2008).

The averaged (over all channels) widths of the forward and aft swaths are 950 (the viewing angle is 68°) and 350 km (23°) (Gaiser et al., 2004). Thus, the requirement imposed by the algorithm under examination (concerning the availability of two measurements of the same surface element at different angles) is satisfied in a narrow (350 km) swath. The sensitivity of radiometric detectors of WindSat with respect to the third and fourth Stokes parameters at 10.7, 18.7, and 37 GHz is 0.25 K (Gaiser et al., 2004).

As was already noted, the same element of resolution on the surface falls within the forward and aft observation sectors after the satellite covers distance $L(\varphi_{31}) = 2R\cos(\varphi_{31})$, where R is the radius of the scan cone on the surface of the Earth, along the track. R = 850 km for WindSat (Gaiser et al., 2004). If we consider the most distant (in time) surface elements (at $\varphi = 0°/180°$), L = 1700 km. This displacement takes place with time delay $\Delta t = L/V$, where V is the low-orbit satellite flight speed, which is roughly equal to 7.5 km/s. Thus, Δt = 226, (6) s, which corresponds to less than 4 m. It was demonstrated in (Monaldo, 1988; Freilich and Dunbar, 1999) that the spatial and temporal mismatch between the measurements from buoys and satellite data may be as large as 50 km and 30 min without any significant loss of measurement accuracy. Therefore, a time delay of 4 min between measurements performed by one and the same instrument should not affect the result.

Calibrated and grid-referenced WindSat measurement data and data on the satellite telemetry and the observation angles (environmental data record) were taken from http://www.ifremer.fr/opendap/cerdap1/oceanflux/satellite/l1/coriolis/windsat in the NetCDF (version 2.0) format. Data on the surface temperature, wind speed, vapor content, precipitation rate, and condensed moisture were taken in the form of maps from http://data.remss.com/windsat/.

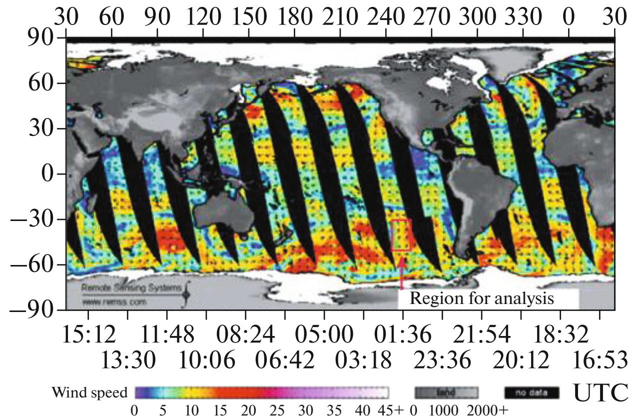

Fig. 6. Map of the wind speed and direction taken from http://data.remss.com/windsat/.

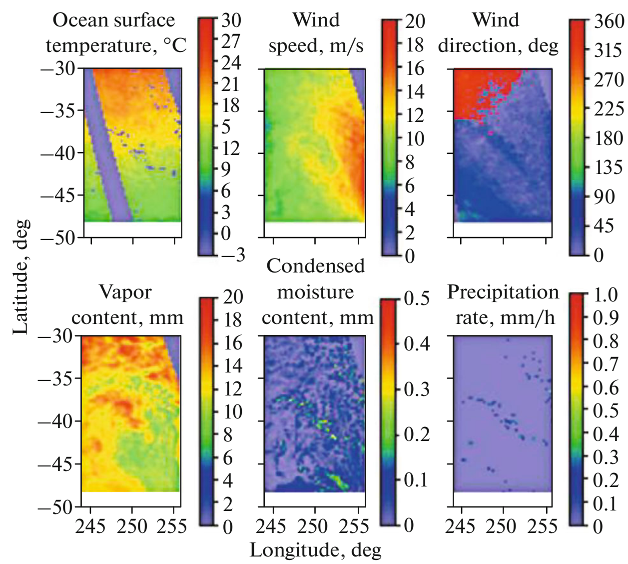

Fig. 7. Geophysical parameters for the test region. http://www.remss.com/missions/windsat/.

CHOOSING A REGION FOR TESTING

The proposed algorithm for determining the wind direction needs to be tested with different combinations of geophysical parameters of the ocean–atmosphere system (i.e., with different water temperatures, values of the atmospheric vapor content, and wind speeds and directions). A small region was selected for testing from the results of measurements performed on April 27, 2007. Figure 6 shows the wind speed and direction map with the testing region highlighted. The geophysical parameters (Fig. 7) of the ocean–atmosphere system vary considerably in this region. Figure 8 shows the measured values of the third Stokes parameter and the azimuthal observation angle for the forward and aft swaths.

Since one and the same surface needs to be measured at different angles to determine the wind direction, the resulting swath used to reconstruct the wind parameters is narrower than both the forward and the aft WindSat swaths. In addition, only the areas with available data on the geophysical parameters of the ocean–atmosphere system are used to solve the problem, since these data are needed to calculate the model dependence of the third Stokes parameter on the relative wind direction. Errors associated with the determination of geophysical parameters and the modeling are neglected (only the instrument sensitivity is taken into account).

All the parameters in Figs. 7 and 8 are referenced to a uniform 0.25° grid (for convenience), but data with accurate coordinate values are used in calculations.

The direct problem (modeling of the azimuthal dependence of the third Stokes parameter (Fig. 1)) is solved by calculating radio brightness temperatures,

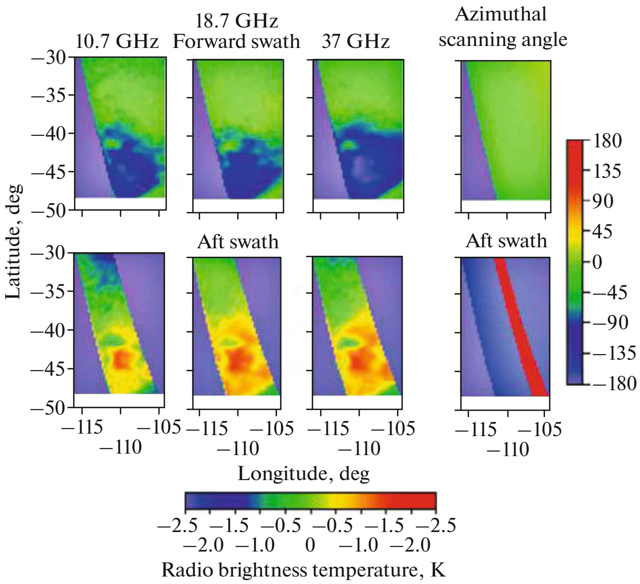

Fig. 8. Radio brightness temperature at three frequencies and azimuthal viewing angles of the WindSat instrument. http://www.ifremer.fr/opendap/cerdap1/oceanflux/satellite/l1/coriolis/windsat.

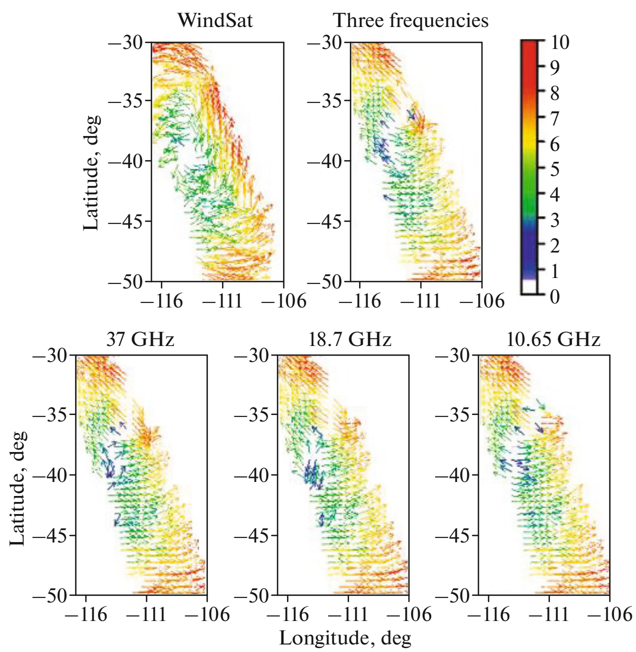

Fig. 9. Results of a reconstruction of the wind direction based on the WindSat measurements of the third Stokes parameter.

which may be measured by a satellite at the given geophysical parameters of the ocean–atmosphere system and scanning parameters. The radio brightness temperatures at linear ±45° polarizations are calculated in accordance with the model of radiothermal radiation of the ocean and the atmosphere, which was developed based on the results of a long-term analysis of satellite data and is described in (Wentz and Meissner, 2000; Meissner and Wentz, 2004, 2012).

Data from the chosen region were analyzed four times (Fig. 9) with the proposed algorithm. The first three calculations were performed for individual frequencies. In the fourth calculation, the wind direction was determined based on the maximum of the resulting probability function for all channels.

DISCUSSION

The results are presented in Fig. 9 in the form of vector maps of the wind direction, where different colors represent different directions. It can be seen that, in some areas, the determined wind direction agrees with the data (product) presented at http://www.remss.com/missions/windsat/. In other areas, the mismatch is considerable. It should be noted that, since in situ measurements for the entire region are not available, the comparison between the reconstructed wind direction and the product was qualitative.

For example, the wind direction in the area with a latitude of –50° to –45° and a longitude of –112° to –106°, reconstructed based on the measurements at individual frequencies and on their combination, is the same as that in the first map in Fig. 9. The directions also agree (although somewhat less accurately) in the area with a latitude of –45° to –40° and a longitude of –111° to –116°. The wind speed in this area is 3–5 m/s. Since the third Stokes parameter is proportional to the wind speed, the accuracy of determination of the wind direction decreases as the wind falls. The wind speed in the area with a latitude of –39° and a longitude of –113° is below 3 m/s, and it becomes impossible to unambiguously determine the wind direction (vectors are directed differently in the figure).

The wind direction in the area with a latitude of –32° to –45° and a longitude of –106° to –111° is reconstructed erroneously at all three individual frequencies (and even if they are combined). Such errors are related to the fact that, as is evident from Figs. 7 and 8, the wind in this area is aligned with the observation direction in the forward and aft swaths. It can be seen in Fig. 1, which presents the dependence of the third Stokes parameter on the relative wind direction, that the $S3(\varphi, ...)$ value is close to zero when the wind direction is collinear with the 0° and 180° viewing directions. The wind direction reconstruction is ambiguous in this case.

In order to resolve these uncertainties, one may introduce the comparison with neighboring points (free from such ambiguities) into the procedure of direction determination (i.e., refine the results after solving the inverse problem). Such approaches are widely used in the analysis of satellite measurements.

CONCLUSIONS

The results of tests of the MicRAWinD algorithm for determining the wind direction based on the WindSat radiopolarimeter measurements demonstrate clearly that this algorithm operates efficiently. The wind field was reconstructed rather accurately with the use of both single-frequency radiometric observations and multi-freqeuency measurements. It was demonstrated that a wind field pattern agreeing in general with the products offered by RSS (http://www.remss.com) may be obtained even without the application of special correction methods.

In addition, the time required to reconstruct the wind direction on a common PC is comparable to the satellite measurement time. This implies the possibility of online data processing (if the geophysical parameters of the ocean–atmosphere system are known (were reconstructed with the use of other fast algorithms)).

Several weeks (months) of measurements need to be processed to obtain quantitative estimates. Although the processing time is comparable to the satellite measurement time, the algorithm still operates rather slowly if applied to a large volume of data. Naturally, this study is already underway; its results will be published separately.

FUNDING

This study was supported by the Russian Foundation for Basic Research, grant no. 18-02-01009.

REFERENCES

Bespalova, E.A., Veselov, K.M., Glotov, A.A., Militskii, Yu.A., Mirovskii, V.G., Pokrovskaya, I.V., Popov, A.E., Raev, M.D., Sharkov, E.A., and Etkin, V.S., Study of wind wave anisotropy by variations of polarized thermal radiation, *Dokl. Akad. Nauk SSSR*, 1979, vol. 246, no. 6, pp. 1482–1485.

Bespalova, E.A., Veselov, V.M., Gershenzon, V.E., Militskii, Yu.A., Mirovskii, V.G., Pokrovskaya, I.V., Raev, M.D., Semin, A.G., Smimov, N.K., Skachkov, V.A., Trokhimovsky, Yu.G., Khapin, Yu.B., Chistyakov, V.N., Sharkov, E.A., and Etkin, V.S., Determination of surface wind velocity from measured polarized anisotropy of intrinsic and scattered microwave radiation, *Issled. Zemli Kosmosa*, 1982, no. 1, pp. 87–94.

Freilich, M.H. and Dunbar, R.S., The accuracy of the NSCAT 1 vector winds: Comparisons with national data buoy center buoys, *J. Geophys. Res.*, 1999, vol. 104, pp. 11231–11246.

Gaiser, P.W., St. Germain, K.M., Twarog, E.M., Poe, G.A., Purdy, W., Richardson, D., Grossman, W., Jones, W.L., Spencer, D., Golba, G., Cleveland, J., Choy, L., Bevilacqua, R.M., and Chang, P.S., The WindSat spaceborne polarimetric microwave radiometer: Sensor description and early orbit performance, *IEEE Trans. Geosci. Remote Sens.*, 2004, vol. 42, no. 11, pp. 2347–2361.

Meissner, T. and Wentz, F.J., The complex dielectric constant of pure and sea water from microwave satellite observations, *IEEE Trans. Geosci. Remote Sens.*, 2004, vol. 42, no. 9, pp. 1836–1849.

Meissner, T. and Wentz, F.J., The emissivity of the ocean surface between 6 and 90 GHz over a large range of wind speeds and earth incidence angles, *IEEE Trans. Geosci. Remote Sens.*, 2012, vol. 50, no. 8, pp. 3004–3026.

Monaldo, F., Expected differences between buoy and radar altimeter estimates of wind speed and significant wave height and their implications on buoy-altimeter comparisons, J. Geophys. Res., 1988, vol. 93, pp. 2285–2303.

Narvekar, P.S., Heygster, G. and Tonboe, R., Analysis of WindSat data over Arctic sea ice, Final version, Technical report for the EUMETSAT satellite application facility on ocean and sea ice, Vis. Sci. Activity SG08-VSQ1: Investigations into use of passive polarimetric microwave radiometry for sea ice retrieval, Rev. 1, Bremen, 2008.

Sadovskii, I.N. and Sazonov, D.S., Determination of the modulus of surface wind velocity from data of the MIRS multifrequency radiometer-spectrometer, *Pyatnadtsataya vserossiiskaya otkrytaya ezhegodnaya konferentsiya “Sovremennye problemy distantsionnogo zondirovaniya Zemli iz kosmosa”. Tezisy dokladov* (Book of Abstracts of the Fifteenth All-Russian Open Annual Conference “Current Problems of the Earth’s Remote Sensing from Space”), Moscow: IKI RAN, 2017, p. 501.

Sazonov, D.S., Azimuthal variability of the radio emission wavy water surface on the basis of microwave measurements, *Pyatnadtsataya vserossiiskaya otkrytaya ezhegodnaya konferentsiya “Sovremennye problemy distantsionnogo zondirovaniya Zemli iz kosmosa”. Tezisy dokladov* (Book of Abstracts of the Fifteenth All-Russian Open Annual Conference “Current Problems of the Earth’s Remote Sensing from Space”), Moscow: IKI RAN, 2017, p. 301.

Sazonov, D.S., Kuzmin, A.K., and Sadovskii, I.N., Study of azimuthal anisotropy of intrinsic radio thermal radiation of wavy water surface in CAPMOS experiments, *Preprint of Space Research Inst., Russ. Acad. Sci.*, Moscow, 2013, no. Pr-2170, p. 23.

Sharkov, E.A., Scientific tasks of the *Konvergentsiya* space experiments in the Russian Segment of the International Space Station, *Pyatnadtsataya vserossiiskaya otkrytaya ezhegodnaya konferentsiya “Sovremennye problemy distantsionnogo zondirovaniya Zemli iz kosmosa”. Tezisy dokladov* (Book of Abstracts of the Fifteenth All-Russian Open Annual Conference “Current Problems of the Earth’s Remote Sensing from Space”), Moscow: IKI RAN, 2017, p. 468.

Sterlyadkin, V.V., Sazonov, D.S., Pashinov, E.V., and Kuzmin, A.V., Description of the algorithm for determining the surface wind direction by radiometric measurements from space, *Pyatnadtsataya vserossiiskaya otkrytaya ezhegodnaya konferentsiya “Sovremennye problemy distantsionnogo zondirovaniya Zemli iz kosmosa”. Tezisy dokladov* (Book of Abstracts of the Fifteenth All-Russian Open Annual Conference “Current Problems of the Earth’s Remote Sensing from Space”), Moscow: IKI RAN, 2017, p. 468.

Wentz, F.J. and Meissner, T., *AMSR Ocean Algorithm, Version 2, Tech. Rep.* 121599A-1, Santa Rosa, Calif.: Remote Sensing Systems, 2002. http://www.remss.com/papers/amsr/AMSR_Ocean_Algorithm_Version_2.pdf.

Translated by D. Safin